

Rigidities of Cationic Surfactant Films in Microemulsions

Julian Eastoe* and Donal Sharpe

School of Chemistry, University of Bristol, Bristol BS8 ITS, U.K.

Richard K. Heenan

ISIS Facility, Rutherford Appleton Laboratory, Chilton, Oxon OX11 0QX, U.K.

Stefan Egelhaaf

ILL, BP 156-X, Grenoble F-38042 Cedex, France

Received: July 10, 1996; In Final Form: October 5, 1996[⊗]

The bending rigidities of dichain cationic surfactant monolayers in Winsor II water-in-cyclohexane microemulsions have been studied using surface light scattering (SLS) and small-angle neutron scattering (SANS). The elastic moduli ($2K + Kbar$) are typically between 1.0 and 2.5 $k_B T$ and increase with both surfactant chain length and added NaBr electrolyte. For salt free systems the scaling relationship observed with surfactant film thickness t , $2K + Kbar \sim t^{2.3}$, agrees reasonably well with theory. The separate electrostatic contribution $(2K + Kbar)_{elec}$ has been calculated using known equations, and this has been used to provide estimates for inherent surfactant rigidities $(2K + Kbar)_{surf}$. This work shows that the film bending elasticity model is a valid description of these microemulsions.

Introduction

The Helfrich film bending energy model¹ has been applied to describe microemulsion properties, and a review article² summarises recent theoretical and experimental work. This approach considers characteristic elastic moduli of the film K and $Kbar$: K is the mean bending modulus which should always be positive, while $Kbar$ is the Gaussian modulus, and in the case of spherical droplet structures it is expected to be negative. The motivation for this work was to apply the model to films in water-in-oil microemulsions to determine the bending elasticities $(2K + Kbar)$ for a series of dichained ionic surfactants.

At a low volume fraction ϕ of spherical droplets the free energy F per unit area of microemulsion interface A may be written in terms of two separate film bending F_b and entropic F_{ent} contributions³

$$\frac{F}{A} = F_b + F_{ent} = \left\{ 2K \left(\frac{1}{R} - \frac{1}{R_0} \right)^2 + \frac{Kbar}{R^2} \right\} + \left\{ \left(\frac{k_B T}{4\pi R^2} \right) f(\phi) \right\} \quad (1)$$

The parameters R and R_0 represent the radius and the preferred radius respectively, while $f(\phi)$ accounts for the entropy of mixing of the microemulsion droplets. For $\phi < 0.1$ it has been shown that the function $f(\phi)$ is adequately given by $\{\ln(\phi) - 1\}$,³ and this approximation is used here. The microemulsion phase behavior can be readily manipulated so that there is a coexistence of dispersed phase with the microemulsion: Winsor I systems for oil-in-water (o/w) and Winsor II systems for water-in-oil (w/o). In these situations R is the maximum radius R_m , and minimization of the total free energy leads to⁴

$$\frac{R_m}{R_0} = \frac{(2K + Kbar)}{2K} + \left(\frac{k_B T}{8\pi K} \right) f(\phi) \quad (2)$$

Although it is difficult to measure K and $Kbar$ separately, this

has been done recently for AOT² and SDS/alcohol films⁵ in microemulsions.

The combination $2K + Kbar$ may be obtained if both R_m and the interfacial tension between the two phases γ_0 are known⁶

$$2K + Kbar = \gamma_0 R_m^2 - \frac{k_B T}{4\pi} f(\phi) \quad (3)$$

Owing to thermal fluctuations the droplets are polydisperse, and it is now known that a distribution in droplet size (as opposed to shape) is the principal cause.³ A Schultz function, with a mean core radius R_m^{av} , can be used to describe the polydispersity, and for this case the width σ/R_m^{av} is related to $2K + Kbar$ by

$$2K + Kbar = \frac{k_B T}{8\pi(\sigma/R_m^{av})^2} - \frac{k_B T}{4\pi} f(\phi) \quad (4)$$

Hence independent measurements of γ_0 , by surface light scattering (SLS) or spinning drop tensiometry (SDT), R_m , and polydispersity by small-angle neutron scattering (SANS), may be combined to obtain $2K + Kbar$. Gradzielski *et al.* have recently used this approach in a systematic study of nonionic surfactants in Winsor I systems.³ However, less is known about cationic surfactants.

Previously SANS has been used to study droplet structure in salt-free Winsor II systems formed by *n*-alkyl-*n*-dodecyldimethylammonium bromide (C_n -C12) surfactants, as a function of the chain length C12 to C18.^{7,8} The SANS data from a contrast variation series were analyzed simultaneously together in terms of a Schultz distribution of core-shell particles. This method is also used here, since it is believed to yield the most representative structural parameters.^{7,8} In the present paper the elasticities $2K + Kbar$, as a function of both surfactant chain length and added NaBr electrolyte, were obtained from SLS and SANS measurements on Winsor II microemulsions. The work is the first systematic study of cationic surfactant microemulsions in terms of the film bending energy model.

[⊗] Abstract published in *Advance ACS Abstracts*, January 1, 1997.

Experimental Section

Chemicals. The *n*-alkyl-*n*-dodecyldimethylammonium bromides (C12–C12, C14–C12, C16–C12, and C18–C12) were prepared, purified and analyzed as described previously.⁷ The C12–C12 surfactant is commercially available as DDAB. All surfactants were stored over refreshed P₂O₅ in a desiccator cabinet until used. Cyclohexane-*d*₁₂ and D₂O, both from CDN Isotopes, contained >99% D-atom. Cyclohexane-*h*₁₂ was obtained from Aldrich and columned over alumina before use. H₂O was doubly distilled, and NaBr was Aldrich ACS grade (99+%).

The microemulsion phase equilibria were determined as described previously,⁷ and the parameter w is given by [water]/[surfactant]. The Winsor II systems consisted of a w/o microemulsion, at a maximum value w_{\max} , in equilibrium with excess aqueous phase. At 25 °C, in salt-free systems w_{\max} was 12.0 for C12 and C14, ~11.0 for C16, and 10.5 for C18. Replacing H₂O with D₂O, or C₆H₁₂ with C₆D₁₂, had no noticeable effect on w_{\max} .

Small-Angle Neutron Scattering. The SANS experiments used the time-of-flight LOQ (ISIS, U.K.), and also the steady-state D17 diffractometer at ILL (Grenoble, France), to determine the scattering probability $I(Q)$ (cm⁻¹). The neutron momentum transfer Q is given by $(4\pi/\lambda)\sin(\theta/2)$ with λ the incident neutron wavelength (2.2 → 10 Å at ISIS and 9.3 Å at ILL) and θ the scattering angle. These conditions gave a useful Q -range of 0.02 → 0.20 Å⁻¹ on LOQ and 0.025 → 0.29 Å⁻¹ on D17. Instrument calibration determined the absolute intensity to better than ±5%. The accepted procedures for data normalization, reduction, and background were carried out (e.g., see ref 7). All samples were thermostated at 25 ± 0.2 °C, and upper w/o portions (~99% of the volume) of the Winsor II systems were illuminated by the neutron beams.

A contrast series was studied for certain systems: core contrast D₂O/H-*n*-C/C₆H₁₂ (D/H/H); shell contrast D₂O/H-*n*-C/C₆D₁₂ (D/H/D); droplet contrast H₂O/H-*n*-C/C₆D₁₂ (H/H/D). Further details concerning the SANS analysis can be found in refs 7 and 8. Since the scattering length densities ρ and concentrations of the components are all known, the four parameters fitted to the three data sets were R_m^{av} , σ/R_m^{av} as well as the apparent film thickness t and scattering length density ρ_{film} . The individual data sets can also be analyzed on their own, but very similar polydispersities are obtained.⁸ Instrumental resolution is taken into account in the modeling.

Interfacial Tension Measurements. The interfacial tensions between the microemulsion and excess aqueous phases γ_0 were measured at 25 ± 0.1 °C using an SLS rig described previously,⁹ and also a Krüss SITE 04 spinning drop tensiometer. For the SLS measurements Winsor II samples were preequilibrated; then the two phases were carefully recombined into 20 mm diameter cylindrical Hellma cells. SLS experiments were performed only when the samples exhibited a mirrorlike macroscopic interface. In order to obtain γ_0 the SLS data were analyzed using the method of Earnshaw et al.,¹⁰ modified for the presence of two bulk liquid phases of different density and viscosity.¹¹ To determine γ_0 a range of wavevectors (200 < q < 900 cm⁻¹) were studied and there was no obvious q -dependence. Further details about SLS can be found elsewhere.¹¹ No changes in γ_0 over a period of up to 2 weeks were noticed, and agreement between SLS and SDT was always better than ±10%. In this paper only the SLS data are presented where the reproducibilities and uncertainties in γ_0 are better than 2%.

Results and Discussion

1. Variation of Surfactant Chain Length. Firstly the effects of increasing the surfactant chain length on the film are discussed.

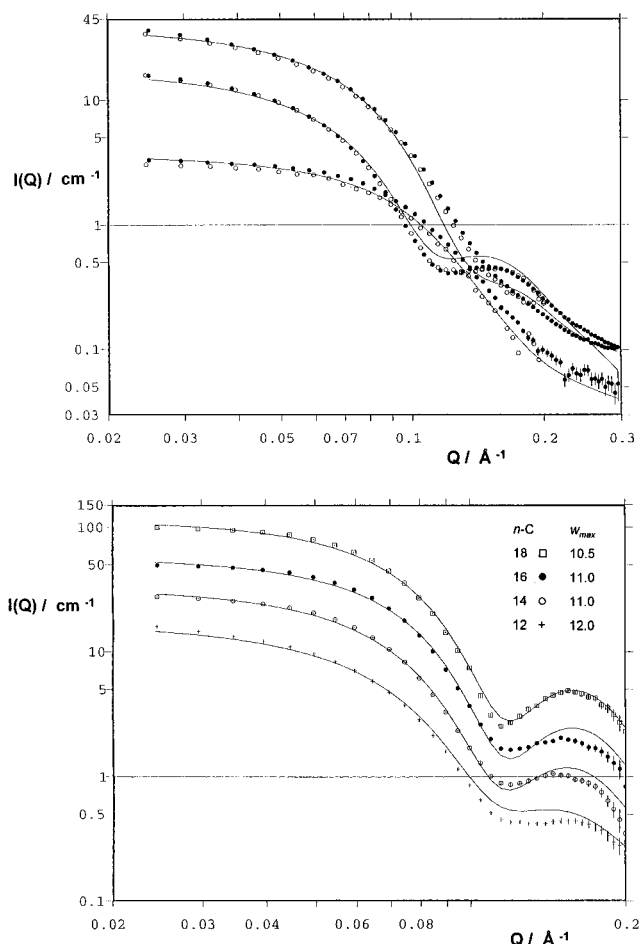


Figure 1. SANS data and analysis for Winsor II microemulsions. Temperature 25 ± 0.2 °C, surfactant concentration 0.10 mol dm⁻³. The fitted parameters are given in Table 1. (a, top) C12–C12 (DDAB) surfactant, with increasing intensity at low Q are core (D/H/H), shell (D/H/D), and drop (H/H/D) contrasts. Volume fractions: $\phi_{\text{water}} = 0.0216$, $\phi_{\text{surf}} = 0.0462$, $w_{\max} = 12.0$. Data from LOQ (○) and D17 (●). Error bars shown for D17 data only. (b, bottom) Shell contrast with increasing chain length n -C. Each data set and the corresponding simultaneous fit is multiplied by an arbitrary constant: C12 (+); C14 × 2 (○); C16 × 4 (●); C18 × 8 (□). Data measured using LOQ, error bars as shown.

TABLE 1: Values Obtained from SANS Data Analysis of Winsor II Microemulsions at Surfactant Concentration = 0.10 mol dm⁻³ and 25 °C^a

surfactant	$R_m^{\text{av}}/\text{Å}$	$t/\text{Å}$	$\rho_{\text{film}}/10^{10} \text{ cm}^{-2}$	σ/R_m^{av}	$2K + K_{\text{bar}}/k_B T$
C12	19.7	11.0	-0.40	0.25	1.08
C14	18.1	11.7	0	0.24	1.13
C16	17.8	12.8	+0.12	0.20	1.44
C18	18.6	13.5	+0.25	0.18	1.68

^a Parameters: t and ρ_{film} are apparent shell thickness and scattering length density; R_m^{av} , average radius of water core; σ/R_m^{av} width of Schultz distribution function. The bending energies ($2K + K_{\text{bar}}$) were calculated using eq 4. Uncertainties in dimensions are ±1 Å, and film rigidities not more than 10%.

Droplet Structure and Polydispersity. The SANS data in core, shell, and drop contrast with the C12–C12 (DDAB) surfactant are shown in Figure 1a. The fitted curves are also displayed, and the fit parameters given in Table 1. As shown previously, there is no clear evidence for any discrete water mixing into the headgroup region, the penetration of cyclohexane into the layer is minimal, and the scattering length density profile across the film is best described by a sharp-step model.^{7,8} Since these data are for two different sets of samples, measured on two different types of SANS instruments, the agreement is good.

Furthermore, no significant differences in the fitted parameters were observed between the LOQ and D17 data. The same was true for similar samples of the C18–C12 surfactant which were also checked in this way.

In core contrast the mean area per headgroup a_h may be estimated from the high- Q asymptote of a Porod plot ($\{I(Q)/Q^4\}$ vs Q) (e.g., see ref 12). For all the n -C surfactants the values of a_h were very similar, and any differences within the uncertainties.⁷ A higher Q was accessible on D17, and for this purpose these measurements are expected to be more reliable: the analyses gave $a_h = 76 \pm 8 \text{ \AA}^2$. In comparison the LOQ experiments gave $65 \pm 15 \text{ \AA}^2$. These values are close to the 68 \AA^2 per headgroup obtained from X-ray scattering measurements from the lamellar phase of C12–C12 (DDAB).¹³ This suggests that the neutral surface (the one that suffers no change in area as the film is unbent) is close to the headgroup region. Therefore, to a good approximation, the fitted water core radius R_m^{av} may be identified with the maximum radius R_m in eqs 2 and 3.

The shell contrast data, and simultaneous fits using the core–shell–drop model, for samples of C12, C14, C16, and C18 surfactants at w_{max} are shown on Figure 1b. (The corresponding data and fits for the core and drop contrasts have been left out, but the fit qualities were very similar to those shown on Figure 1a.) The fitted parameters are given in Table 1. Since w_{max} was similar for the different surfactants, little variation in R_m^{av} was observed. As expected, the apparent film thickness t increases with carbon number, although it is always around 60–65% of an all *trans* chain. As shown previously,^{7,8} the changes in ρ_{film} are consistent with an increase in penetration of C_6D_{12} into the layer: for C12 (DDAB) and C18 the apparent volume fraction in the film $\Phi_{\text{C}_6\text{D}_{12}}$ increases from essentially zero to 0.08.

In shell contrast a lower polydispersity gives rise to a sharper first minimum in the $I(Q)$ profile.⁷ It is clear from Figure 1b that as the surfactant chain length increases, the polydispersity decreases, and this is quantified by the fitted values for σ/R_m^{av} given in Table 1.

Interfacial Tensions and Film Elasticities. The cyclohexane-continuous microemulsion-excess aqueous phase interfacial tensions γ_0 are shown on Figure 2 as a function of surfactant chain length n -C. It is interesting to compare these results with single chain surfactants at the air–water interface, where above the critical micelle concentrations (cmc's) γ_0 will generally decrease with n -C.¹⁴ However, as described below, the increase in γ_0 observed here is entirely consistent with the bending energy model.

Figure 3 shows the bending elasticities ($2K + \text{Kbar}$) as a function of surfactant chain length, calculated using measured values of γ_0 , R_m^{av} , and σ/R_m^{av} and either eq 3 or 4. The results from the polydispersity analysis alone are given in Table 1. The propagated uncertainties in $2K + \text{Kbar}$ are not more than $\pm 10\%$, and as can be seen, there is good agreement between the two methods.

For constant droplet size R_m and volume fraction ϕ , eqs 3 and 4 predict that an increase in $2K + \text{Kbar}$ should go hand in hand with an increase in γ_0 and decrease in droplet polydispersity. On theoretical grounds increasing the surfactant chain length is expected to increase the film rigidity.¹⁵ The measured bending elasticities scale in a similar way with either film thickness t or the total number of alkyl chain carbons N , so that $2K + \text{Kbar} \sim t^{2.3} \sim N^{2.3}$. A similar exponent has been found experimentally for C_iE_j surfactants in Winsor I systems,³ and also theoretically¹⁵ on the basis of hydrocarbon chain packing statistics for K only (for which it is 2.5–3).

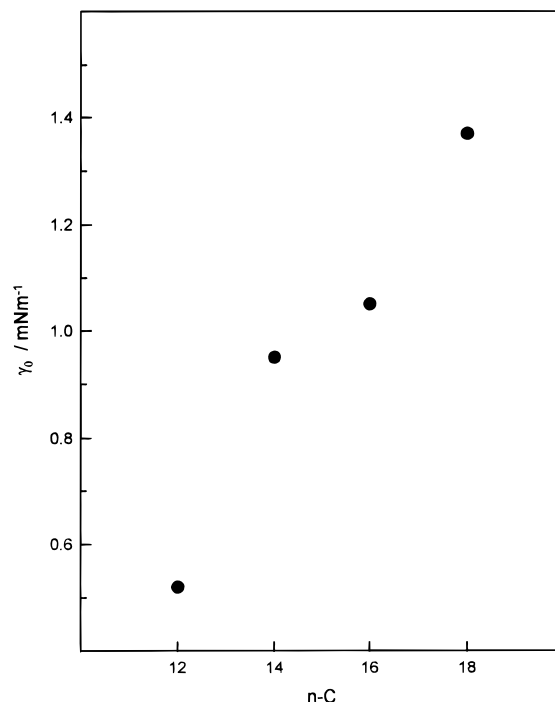


Figure 2. Interfacial tensions γ_0 , measured by SLS, in Winsor II systems as a function of surfactant chain length n -C.

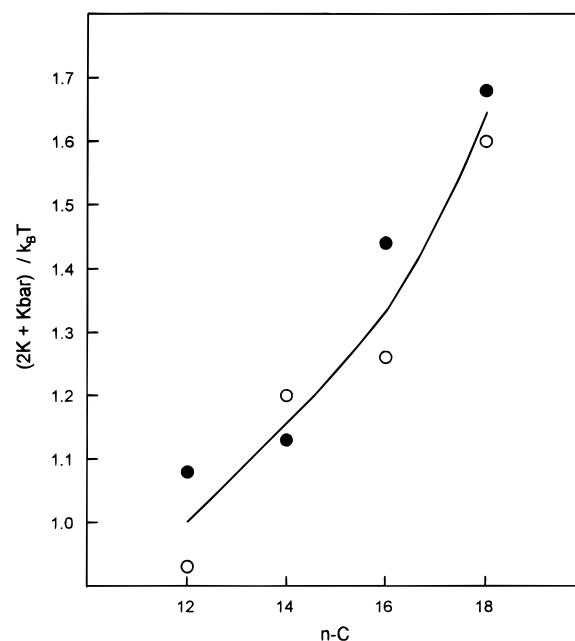


Figure 3. Surfactant film elasticities $2K + \text{Kbar}$, in units of $k_B T$, as a function of surfactant chain length n -C. The line is a guide to the eye. $2K + \text{Kbar}$ was calculated using γ_0 and R_m measured by SLS and SANS and eq 3 (○) and σ/R_m^{av} determined from SANS analyses and eq 4 (●).

The effects of surfactant concentration were also checked. It has been established in previous work⁷ that for these systems at w_{max} the internal droplet structure and polydispersity are invariant over the range [surfactant] $0.025 \rightarrow 0.15 \text{ mol dm}^{-3}$ (i.e., water volume fraction ϕ , $0.0054 \rightarrow 0.0324$). Over this range the tensions γ_0 were also very similar, and any changes in $2K + \text{Kbar}$ as calculated by eq 3 were within the $\pm 10\%$ uncertainty.

2. Variation of NaBr Concentration. The effects of added NaBr on the film rigidity are now considered.

Droplet Radii and Interfacial Tensions. Increasing the electrolyte concentration over the range $0 \rightarrow 0.10 \text{ mol dm}^{-3}$ NaBr

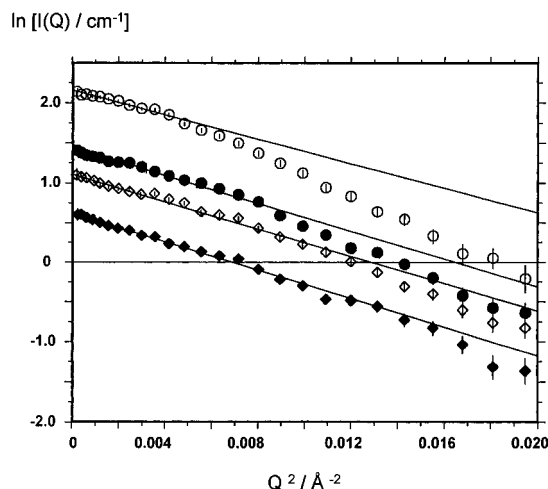


Figure 4. Effect of NaBr concentration on SANS from Winsor II microemulsion droplets with C12–C12 (DDAB) surfactant in core (D/H/H) contrast. Fits are to the low- Q region data ($<0.07 \text{ \AA}^{-1}$) using the Guinier law for spherical particles: temperature, $25 \pm 0.2 \text{ }^\circ\text{C}$, surfactant concentration, 0.10 mol dm^{-3} . Error bars as shown. $[\text{NaBr}]/\text{mol dm}^{-3}$: 0.0 (○); 0.0125 (●); 0.025 (◇); 0.10 (◆). For presentation purposes some of the data and fitted lines are displaced by an arbitrary constant: +1.5, +0.75, and 0.5 for the 0, 0.0125, and 0.025 mol dm^{-3} NaBr, respectively.

had little effect on either w_{max} or the droplet size. Figure 4 shows a Guinier representation of the SANS data for Winsor II droplet systems in core (D/H/H) contrast with C12–C12 surfactant, at four example electrolyte concentrations. The water radius R_m can be estimated from the gradient of a fit to the low- Q data (e.g., see ref 16): the radii are 19.6, 20.9, 20.8, and 21.2 \AA for the 0, 0.125, 0.025, and 0.10 mol dm^{-3} NaBr samples, respectively. The value of 19.6 \AA for the salt-free sample, derived from this Guinier approximation, agrees well with that obtained by the more sophisticated analysis (see Table 1).

Similar behavior was found for the C14 and C18 surfactants up to 0.10 mol dm^{-3} electrolyte. When the data for C12–C12 were analyzed using the Schultz core model σ/R_m^{av} decreased from 0.25 without salt to about 0.17 for the highest concentration. From eq 4 this is consistent with an increase in $2K + \text{Kbar}$ from approximately 1.1 to $1.7 k_B T$. It was not possible to study these systems in the three separate core–shell–drop contrasts as a function of electrolyte, and the polydispersities could not be determined with as much confidence as for the salt-free cases. However, it is clear from Figure 4 that droplet size and shape are not significantly affected by NaBr concentration up to 0.10 mol dm^{-3} . This result is initially puzzling, since the effects of electrolyte on the structure of anionic surfactant microemulsions are well-documented (see ref 17). For these droplets the radius is $\sim 20 \text{ \AA}$, making the local concentration of Br^- surfactant counterions in the water pool about 3.3 mol dm^{-3} , resulting in a Debye length $\kappa^{-1} \sim 2 \text{ \AA}$. In the pools, addition of electrolyte will reduce κ^{-1} further still, and therefore little effect on the droplet radius is expected. From the absolute SANS intensities it could be seen that the aqueous phase volume fraction ϕ remained essentially constant over this range of salt concentration.

The tensions at the planar microemulsion–aqueous phase interface increased consistently up to 0.10 mol dm^{-3} added NaBr, and the maximum change was $\sim 2 \text{ mN m}^{-1}$ above γ_0 of the salt-free systems. For constant ϕ and R_m , eq 3 predicts that γ_0 should increase with film rigidity $2K + \text{Kbar}$. Since the tensions could be determined more reliably than the polydispersities, γ_0 values were used to obtain the film bending energies as a function of salt concentration.

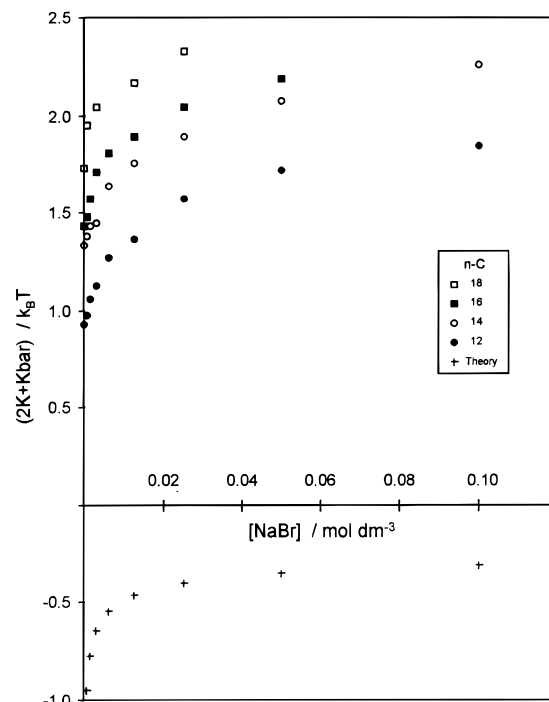


Figure 5. Film rigidities $2K + \text{Kbar}$ as a function of NaBr concentration and surfactant chain length $n\text{-C}$: temperature, $25 \pm 0.1 \text{ }^\circ\text{C}$; surfactant concentration, 0.05 mol dm^{-3} . $2K + \text{Kbar}$ was calculated using eq 3. The theoretical values of $2K + \text{Kbar}_{\text{elec}}$, shown by +, were calculated using eq 5. $n\text{-C}$: 12 (●); 14 (○); 16 (■); 18 (□).

Film Elasticities. Figure 5 shows the values for $2K + \text{Kbar}$ as a function of both electrolyte concentration and chain length, calculated using measured values of γ_0 , R_m , and eq 3. The changes in $2K + \text{Kbar}$ are principally due to the observed increase in γ_0 . The increase in $2K + \text{Kbar}$ for the C12–C12 surfactant is consistent with the decrease in σ/R_m^{av} that was noted above.

For ionic surfactants the overall film elasticity may be considered in terms of a constant “natural” surfactant $(2K + \text{Kbar})_{\text{surf}}$ contribution, separate from a salt-dependent electrostatic part $(2K + \text{Kbar})_{\text{elec}}$. Theories accounting for the effect of electrolyte on $(2K + \text{Kbar})_{\text{elec}}$ have been proposed by Mitchell and Ninham¹⁸ and Lekkerkerker.¹⁹ The two approaches are slightly different, but the authors identify two limiting regimes, high and low surface charge density corresponding to low and high bulk electrolyte concentrations. For the present situations, $[\text{NaBr}] \leq 0.10 \text{ mol dm}^{-3}$ and the high charge density approximation is appropriate.^{18,19} The surfactant surface charge density σ was taken to be $\approx 0.21 \text{ C m}^{-2}$ ($e/a_h \approx \{1.69 \times 10^{-19} \text{ C}/(7.5 \times 10^{-19} \text{ m}^2)\}$). These calculations gave negative values of $(\text{Kbar})_{\text{elec}}$ and the composite term $(2K + \text{Kbar})_{\text{elec}}$. The values obtained using the Mitchell–Ninham equation are included in Figure 5:

$$(2K + \text{Kbar})_{\text{elec}} = \frac{2\epsilon(k_B T)^2}{\pi\kappa e} \left\{ 1 - \left[\frac{\pi^2}{6} + \kappa t \ln\left(\frac{s}{4}\right) \right] \right\} \quad (5)$$

where ϵ is the dielectric constant for water, κ is the inverse Debye length, e is the electronic charge, and t is the film thickness.¹⁸ The parameter s is given by $4\pi e\sigma/(\epsilon\kappa k_B T)$. For electrolyte concentrations lower than $0.025 \text{ mol dm}^{-3}$ the other approach¹⁹ gave a steeper dependence than was suggested by the measurements. However, when the $2K + \text{Kbar}$ values for $0.025 < [\text{NaBr}] < 0.10 \text{ mol dm}^{-3}$ for C12 and C14 were plotted vs $[\text{NaBr}]^{-1/2}$, a slope of -0.085 was found. This is very close

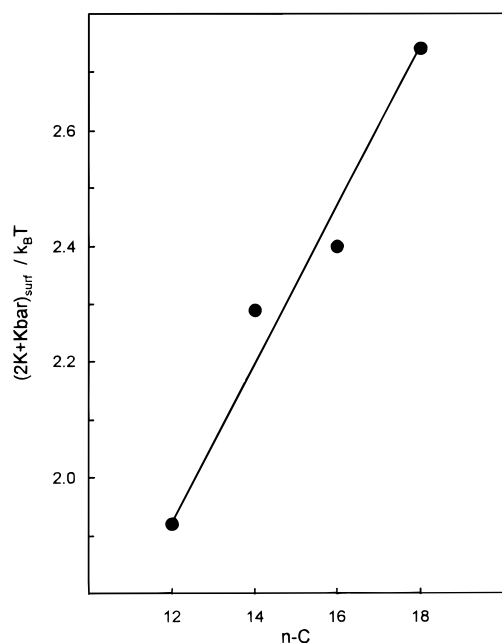


Figure 6. Surfactant rigidities $(2K + Kbar)_{surf}$ as a function of surfactant chain length n -C. The line is a guide to the eye.

to Lekkerkerker's prediction of -0.09 .¹⁹ In any case over this concentration range the two theories predict very similar rigidities.²⁰

As can be seen in Figure 5, there is essentially a constant difference between the measured $2K + Kbar$ and the calculated $2K + Kbar_{elec}$, especially for electrolyte concentrations greater than $0.025 \text{ mol dm}^{-3}$. This difference may be attributed to a chain only contribution $(2K + Kbar)_{surf}$.¹⁹ Values for $(2K + Kbar)_{surf}$ derived in this way are plotted on Figure 6, and the increase in rigidity with chain length is as expected. The approximate scaling relations $(2K + Kbar)_{surf} \sim t^{1.5} \sim N^{1.5}$ are found, and this exponent is lower than expected. Obviously the exponent will depend on the model that is used to calculate the electrostatic contribution.

Conclusions

Small-angle neutron scattering and surface light scattering measurements show that bending energy theory provides a good description of the properties of Winsor II microemulsions stabilized by di- n -alkyldimethylammonium bromide surfactants. With no added electrolyte the film rigidities $2K + Kbar$ determined by two different routes are in good agreement. Furthermore, the observed power-law dependence of $2K + Kbar$ on surfactant chain length with exponent ~ 2.3 is similar to recent work on nonionic surfactants in Winsor I systems³ and theoretical predictions for K only.¹⁵ Addition of NaBr electrolyte up to 0.10 mol dm^{-3} increases the rigidity of the film, and this can be accounted for by theory.^{18,19} Using these experimental results and theoretical calculations^{18,19} separate contributions to the overall bending energies, inherent to the

surfactant $(2K + Kbar)_{surf}$ and owing to electrostatics $(2K + Kbar)_{elec}$, were obtained. The part originating from the surfactant only is positive and therefore opposes film bending. The electrostatic contribution is always negative, even at the highest salt concentrations studied here. These results represent the first systematic study of film rigidities for dichain cationic surfactants and should stimulate further theoretical work on the physico-chemical origins of elastic moduli.

Acknowledgment. A BBSRC research grant was awarded to set up the SLS rig, and D.S. thanks BBSRC for a postdoctoral fellowship. Both ISIS U.K. and ILL France are thanked for providing neutron beam time as well as funds for travel and consumables. We warmly thank the following: Jinfeng Dong (University of Hull, U.K.), Karen J. Hetherington (Bristol), and A. James Bloomfield (Bristol) for initial work on the surfactants, microemulsions and spinning drop measurements; Prof. J. C. Earnshaw (Queen's University, Belfast, U.K.) for providing the analysis programs, and Dr. Spence Taylor (BP, Sunbury, U.K.) for donating some equipment. Prof. J. Meunier (Paris) is thanked for his advice.

References and Notes

- (1) Helfrich, W. Z. *Naturforsch.* **1973**, 28C, 693.
- (2) Binks, B. P.; Kellay, H.; Hendriks, Y.; Lee, L. T.; Meunier, J. *Adv. Colloid Interface Sci.* **1994**, 49, 85.
- (3) Gradziński, M.; Langevin, D.; Farago, B. *Phys. Rev. E* **1996**, 53, 3900.
- (4) Safran, S. A. In *Structure and Dynamics of Strongly Interacting Colloids and Supramolecular Aggregates in Solution*; Chen, S.-H., Huang, J. S., Tartaglia, P. Eds.; NATO ASI Series C; Kluwer: Dordrecht, The Netherlands, 1992; Vol. 39.
- (5) Kegel, W. K.; Bodnar, I.; Lekkerkerker, H. N. W. *J. Phys. Chem.* **1995**, 99, 3272.
- (6) Meunier, J.; Lee, L. T. *Langmuir* **1991**, 7, 1855.
- (7) Eastoe, J.; Dong, J.; Hetherington, K. J.; Steytler, D. C.; Heenan, R. K. *J. Chem. Soc., Faraday Trans.* **1996**, 92, 65.
- (8) Eastoe, J.; Dong, J.; Hetherington, K. J.; Steytler, D. C.; Heenan, R. K. *Langmuir* **1996**, 12, 3876.
- (9) Sharpe, D.; Eastoe, J. *Langmuir* **1996**, 12, 2303.
- (10) Earnshaw, J. C.; McGivern, R. C.; McLaughlin, A. C.; Winch, P. *J. Langmuir* **1990**, 6, 649.
- (11) Langevin, D., Ed. *Light Scattering by Liquid Surfaces and Complementary Techniques*; Dekker: New York, 1992.
- (12) Auvray, L.; Auroy, P. In *Neutron and X-Ray Scattering: Introduction to an Investigative Tool for Colloidal and Polymeric Systems*; Lindner, P., Zemb, Th. Eds.; North-Holland: Amsterdam, 1991; p 199.
- (13) Evans, D. F.; Mitchell, D. J.; Ninham, B. W. *J. Phys. Chem.* **1986**, 90, 2817.
- (14) van Os, N. M.; Haak, J. R.; Rupert, L. A. M. *Physico-Chemical Properties of Selected Anionic, Cationic and Nonionic Surfactants*; Elsevier: Amsterdam, 1993.
- (15) Szleifer, I.; Kramer, D.; Ben-Shaul, A.; Gelbart, W. M.; Safran, S. A. *J. Chem. Phys.* **1990**, 92, 6800. Szleifer, I.; Ben-Shaul, A.; Gelbart, W. M. *J. Phys. Chem.* **1990**, 94, 5018. Szleifer, I.; Kramer, D.; Ben-Shaul, A.; Gelbart, W. M.; Roux, D. *Phys. Rev. Lett.* **1988**, 60, 1966.
- (16) Eastoe, J. In *New Physico-Chemical Techniques for the Characterisation of Complex Food Systems*; Dickinson, E., Ed.; Blackie: Glasgow, U.K., 1995; Chapter 12, pp 268–294.
- (17) Clint, J. *Surfactant Aggregation*; Blackie: Glasgow, U.K., 1993; Chapter 10.
- (18) Mitchell, D. J.; Ninham, B. W. *Langmuir* **1989**, 5, 1121.
- (19) Lekkerkerker, H. N. W. *Physica A* **1989**, 159, 319.
- (20) The values for $(2K + Kbar)_{elec}$ were, at $0.025 \text{ mol dm}^{-3}$ NaBr, -0.40 and -0.57 and, at 0.10 mol dm^{-3} , -0.30 and $-0.29 k_B T$ using the approaches of Mitchell and Ninham, and Lekkerkerker, respectively.